

## Robust control of the three-phase voltage-source PWM rectifier using EKF load current observer

**Abstract:** A load current observer using EKF is proposed to compensate the changed load current for a robust dc voltage control without the inconvenient of the current sensor installation in the three-phase voltage-source PWM rectifier. Besides, a simplified model and the EKF observer based on it are also proposed. A small-signal model of the rectifier is also analyzed to prove the rationality of the feed-forward compensation. Simulation and experimental results demonstrate the proposed feed forward compensations with EKF observers based on both the normal and simplified models can improve the dynamic performance of the dc-link voltage satisfyingly.

**Streszczenie.** W artykule przedstawiono zastosowanie obserwatora prądu obciążenia z filtrem EKF, dla trójfazowego prostownika napięcia, celem ulepszenia kompensacji uchybu napięcia DC, bez instalowania czujników prądu. W celu weryfikacji działania układu ze sprzężeniem do przodu i obserwatorem EKF, wykonano badania symulacyjne i eksperymentalne proponowanego rozwiązania, które potwierdziły skuteczność i dynamikę działania. (Obserwator prądu obciążenia oparty na filtrze EKF w sterowaniu trójfazowym prostownikiem napięcia PWM).

**Keywords:** three-phase voltage-source PWM rectifier, EKF, feed-forward compensation, simplified model.

**Słowa kluczowe:** trójfazowy prostownik napięcia PWM, EKF, kompensacja sprzężeniem do przodu, model uproszczony.

### Introduction

In recent years, the three-phase voltage-source pulse width modulated (PWM) rectifier is widely employed in nonconventional energy sources, such as wind energy conversion systems, solar photovoltaic systems [1,2], etc, and upgrades of some traditional adjustable speed drives with the rectifier instead of diode bridge to a better performances of both the currents power sources and the drive systems, thanks to the viable advantages such as bidirectional power flow, low harmonic distortion of line current, regulation of input power factor to unity, adjustment and stabilization of dc-link voltage, reduced dc filter capacitor size, etc. Many global companies such as ABB, Siemens [3,4], etc, have produced their ac/dc/ac converter productions based on the three-phase voltage-source PWM rectifier.

Thanks to the fast developments of power semiconductor devices and digital signal processors (DSPs), which allow fast operation and cost reduction, many novel control strategies have become possible. Direct power control (DPC), which based on instantaneous direct active and reactive power control, and direct current control strategy in d-q synchronous reference frame, which based on current vector orientation with respect to line voltage vector, are two well-known methods on this type of PWM rectifier [5,6]. In more and more high performance industrial systems, the stabilization of dc-link voltage is one of the most essential parts, especially with the load disturbance. In some PWM converter-inverter system, coordinated control methods have been used. Reference [7] proposed a master-slave control method in forcing the converter power to track the inverter power. Reference [8] proposed a control strategy to utilize the inverter dynamics in controlling the converter dynamics. In order to minimize the response delay of the converter current control loop, reference [9] calculate the compensation amount in terms of voltage and inject it at the voltage node. Perfect simulation and experimental results have been obtained, however, only if just one digital signal processing (DSP) is used in the PWM converter-inverter system, these coordinated control strategies can be realized, because the information of the load of the inverter is needed in every converter current cycle. Actually, many PWM converter-inverter systems use two DSP to control the converter and inverter separately for modularization, because the controls of the converter and inverter are relatively independent. Some papers

compensated the dc load distortion with the dc bus current sampled by a current sensor [10]. In the practical devices, copper bars are usually used because of the high current of the dc bus. It is too difficult to install the current sensor.

In order to realize the dc load distortion compensation without the dc bus current sensor, a dc load current observer would be a proper choose. Until now, there are few literatures about the dc bus current of PWM rectifier. But there are a lot of observers about the motor load torque used in drive systems which is very similar to PWM rectifier systems [11-14]. The extended Kalman Filter (EKF) observer is considered as both stable and robust method [15]. And EKF is an optimal estimator in the least-square sense for estimating the states of dynamic nonlinear systems. But EKF is thought to be excessively complex algorithms, which are difficult to implement (especially in the case of fixed-point application) and require huge computational performance [16].

This paper proposed EKF observers based on both the normal two-dimensional model, and the simplified two-dimensional linearization model to simplify the implementation of the observer. Simulation and experimental results show that good performances can be gotten by both proposed EKF observers with proper observer matrices.

### Mathematic model of the three-phase PWM rectifier

The three-phase voltage-source PWM rectifier is shown in Fig. 1. Here,  $e_a, e_b, e_c$  are the amplitude of the ac voltage;  $i_a, i_b, i_c$  are the amplitude of the ac current;  $u_{dc}$  is the dc voltage;  $i_L$  is the load current.

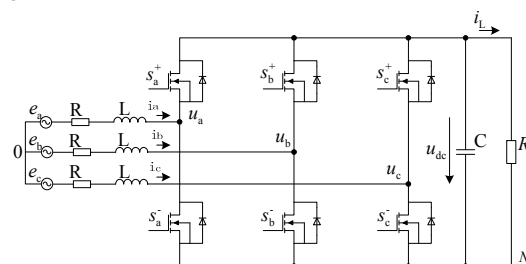


Fig. 1. The three-phase voltage-source PWM rectifier

And  $R$  is the parasitic resistance of the inductance  $L$ ; Parameter  $C$  is the dc filter capacitor; Parameter  $R_L$  is the load in the dc side.

## Synchronous Reference Frame Transformation

The d-q model in the rotating reference frame following phase-locked loop (PLL) of the ac voltage is used to analyze the rectifier, which is expressed as

$$(1) \quad \begin{cases} L \frac{di_d}{dt} + Ri_d = e_d - u_d + \omega Li_q \\ L \frac{di_q}{dt} + Ri_q = e_q - u_q - \omega Li_d \\ C \frac{du_{dc}}{dt} = \frac{3}{2}(i_d s_d + i_q s_q) - i_L \end{cases}$$

where,  $u_d, u_q, i_d, i_q$ , are the voltages and currents of d axis and q axis of the rectifier ac side;  $\omega$  is the electrical speed of the ac voltage.  $e_d, e_q$  are the ac voltage; The ac voltage is fixed on the d axis with PLL, and the ac voltage of q axis is

$$(2) \quad e_q = 0$$

The power balance principle tells that the active power  $p_g$  in the ac input side must be equal to power  $p_{dc}$  in the dc side by ignoring losses causing by the inductors in the ac side and the bridge road of the rectifier.

$$(3) \quad \frac{3}{2}(e_d i_d + e_q i_q) = u_{dc} \left( C \frac{du_{dc}}{dt} + i_L \right)$$

Substituting (2) into (3), the power balancing expression is obtained as

$$(4) \quad \frac{du_{dc}}{dt} = -\frac{i_L}{C} + \frac{3}{2} \frac{e_d}{Cu_{dc}} i_d$$

### Conventional control method

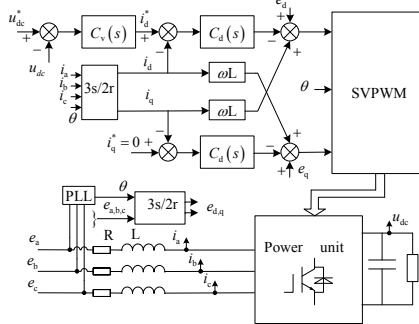


Fig. 2. The conventional control system

The objective of the closed-loop control for the three-phase voltage-source PWM rectifier is to regulate the dc bus voltage to the desired value and synthesize sinusoidal currents with PLL. The structure of the controller based on the direct current control in d-q synchronous reference frame chosen, is shown in Fig. 2. The current-loop and voltage-loop controllers,  $G_d(s)$ ,  $G_q(s)$  and  $G_v(s)$ , are of classical proportional-integral (PI) type.

$$(5) \quad \begin{cases} i_d^* = C_v(s)(u_{dc}^* - u_{dc}) \\ i_q^* = 0 \\ u_d^* = -C_d(s)(i_d^* - i_d) + e_d + \omega Li_q \\ u_q^* = -C_q(s)(i_q^* - i_q) + e_q - \omega Li_d \end{cases}$$

where,

$$(6) \quad \begin{cases} C_v(s) = k_{vp} + \frac{k_{vi}}{s} \\ C_d(s) = k_{dp} + \frac{k_{di}}{s} \\ C_q(s) = k_{qp} + \frac{k_{qi}}{s} \end{cases}$$

The voltage loop controller regulates the dc bus voltage by providing an appropriate d-axis current command to the inner current loop. The q-axis current reference is set to zero to regulate the input power factor to unity

## EKF Observers

If the feed forward load current can be calculated, the dynamic response to load transients can be improved to satisfy the load's wide range. A reasonable method is to estimate the load current directly with the measured dc voltage and ac currents. Then a good-performance filter is needed to satisfy both the fast dynamic response and the measurement noise cancellation. Usually, the good-performance filter is too difficult to obtain. So a high-performance observer such as EKF, which is widely used in the motor load torque observer, is needed.

Considering Equation (4) and treating the load current  $i_L$  as state variable which is constant in the sampling time  $T_s$ , the equation system is expressed as

$$(7) \quad \begin{cases} \frac{du_{dc}}{dt} = -\frac{i_L}{C} + \frac{3}{2} \frac{e_d}{Cu_{dc}} i_d \\ \frac{di_L}{dt} = 0 \end{cases}$$

So the state equations of the system can be written as

$$(8) \quad \begin{cases} dx/dt = Ax + Bu \\ y = Cx \end{cases}$$

$$\text{Here } A = \begin{bmatrix} 0 & -\frac{1}{C} \\ 0 & 0 \end{bmatrix}, \quad B = \begin{bmatrix} \frac{3}{2} \frac{e_d}{Cu_{dc}} \\ 0 \end{bmatrix}, \quad C = [1 \quad 0],$$

$$x = \begin{bmatrix} u_{dc} \\ i_L \end{bmatrix}, \quad u = i_d, \quad y = u_{dc}.$$

### Observability analysis

As we known, EKF is a kind of observer. The observability of the system in Equation (7) or (8) must be considered.

$$(9) \quad \text{rank} \begin{bmatrix} C^T & A^T C^T \end{bmatrix} = \text{rank} \begin{bmatrix} 1 & 0 \\ 0 & -\frac{1}{C} \end{bmatrix} = 2$$

So the system can be observed.

### EKF observer designing

Considering the process noise  $w$  and the measurement noise  $v$ , the system can be written:

$$(10) \quad \begin{cases} dx/dt = Ax + Bu + w \\ y = Cx + v \end{cases}$$

Assuming these noises are stationary, white, uncorrelated and Gauss noises, and their expectation is 0, we define the covariance matrices of these noises:

$$(11) \quad \begin{cases} Q = \text{cov}(w) = E\{ww^T\} \\ R = \text{cov}(v) = E\{vv^T\} \end{cases}$$

To design a digital filter, the continuous time system in Equation (9) can be converted into a discrete time system.

$$(12) \quad \begin{cases} x(k+1) = \Phi_k(x(k), u(k)) + w(k) \\ y(k) = C(k)x(k) + v(k) \end{cases}$$

where,

(13)

$$\Phi_k(x(k), u(k)) = \begin{bmatrix} u_{dc}(k) - \frac{i_L(k)}{C} + \frac{3}{2} \frac{e_d T_s}{Cu_{dc}(k)} i_d(k) \\ i_L(k) \end{bmatrix}$$

And,

$$(14) \quad \frac{\partial \Phi}{\partial x} = \begin{bmatrix} 1 - \frac{3}{2} \frac{e_d T_s}{Cu_{dc}^2(k)} & -T_s/C \\ 0 & 1 \end{bmatrix}$$

So the load current can be estimated following EKF implementation steps.

1. Calculate the next state and the corresponding error.

$$(15) \quad \begin{cases} \hat{x}_{k|k-1} = A(x_{k-1|k-1})x_{k-1|k-1} + B(x_{k-1|k-1})u_{k-1} \\ P_{k|k-1} = \left. \frac{\partial \Phi}{\partial t} \right|_{x=x_{k-1|k-1}} P_{k-1|k-1} \left. \frac{\partial \Phi^T}{\partial t} \right|_{x=x_{k-1|k-1}} - \Phi_{k-1} \end{cases}$$

2. Calculate the Kalman gain.

$$(16) \quad K_k = P_{k|k-1} C^T (C P_{k|k-1} C^T + R_{k-1})^{-1}$$

3. Calculate the best estimate.

$$(17) \quad \hat{x}_{k|k} = \hat{x}_{k|k-1} + K_k (y_k - C \hat{x}_{k|k-1})$$

4. Calculate the best estimate of the error.

$$(18) \quad P_{k|k} = P_{k|k-1} - K_k C P_{k|k-1}$$

$$\text{where, } P_{k|k} = E \{ e_k^T e_k \} = \sum_{i=1}^n E \{ [x_i - \hat{x}_i] [x_i - \hat{x}_i]^T \}$$

### Control strategy with compensation of the load current based on EKF

With the observed load current, the whole control system of the three-phase voltage- sourced PWM rectifier can be operated as Fig. 3.

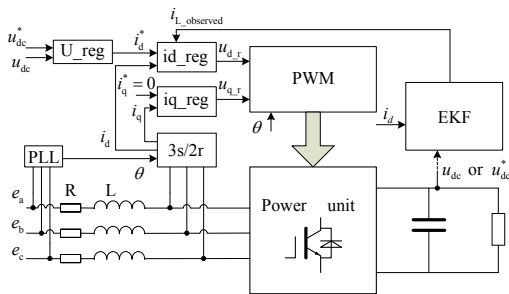


Fig. 3. The proposed control system

In the whole control system shown in Fig.3, a (the phase lock loop) PLL is used to obtain synchronous angle  $\theta$  of the ac voltage.

The dc voltage variation within each control cycle, which is equal to the sampling time  $T_s$  in the system, is considered negligible with respect to the other variable dynamics. To simplify the implantation of the system, the dc voltage  $u_{dc}$  can be replaced by the reference dc voltage  $u_{dc}^*$ . The matrix  $B$  of the equation system in equation (8) can be written as

$$(19) \quad \begin{cases} dx/dt = Ax + B'u \\ y = Cx \end{cases}$$

$$\text{Where, } B' = \begin{bmatrix} \frac{3}{2} \frac{e_d}{Cu_{dc}^*} \\ 0 \end{bmatrix}$$

With the simplified system shown in Equation (7), EKF can also be obtained following the step of the EKF observer based on the normal model.

### Small-signal analysis

To analyze the performance of the proposed control strategy, a small signal model is used. First, the state variables are expressed as the sum of the values at an operating point (large signal) and small deviations from the operating point (small signal) such that

$$(20) \quad \begin{cases} u_{dc} = \bar{U}_{dc} + \tilde{u}_{dc} \\ u_d = \bar{U}_d + \tilde{u}_d \\ i_d = \bar{I}_d + \tilde{i}_d \\ i_L = \bar{I}_L + \tilde{i}_L \end{cases}$$

Where  $\bar{U}_{dc}$ ,  $\bar{U}_d$ ,  $\bar{I}_d$  and  $\bar{I}_L$  denote large signals and  $\tilde{u}_{dc}$ ,  $\tilde{u}_d$ ,  $\tilde{i}_d$  and  $\tilde{i}_L$  denote the corresponding small signals.

With the analysis of the mathematic model of the three-phase voltage-source PWM rectifier, the model can be written as Equation (21), since the analysis is focused on the dc voltage with a changed load.

$$(21) \quad \begin{cases} L \frac{di_d}{dt} = \omega L i_q + e_d - u_d \\ C \frac{du_{dc}}{dt} = \frac{3}{2} \frac{(u_d i_d + u_q i_q)}{u_{dc}} - i_L \end{cases}$$

Substituting Equation (20) into Equation (21), the small-signal model can be written as

$$(22) \quad \begin{bmatrix} \tilde{u}_{dc}(s) \\ \tilde{i}_d(s) \end{bmatrix} = \begin{bmatrix} \frac{3\bar{I}_d L s - 3e_d}{2\bar{U}_{dc} L C s^2} & -\frac{1}{C s} \\ -\frac{1}{L s} & 0 \end{bmatrix} \begin{bmatrix} \tilde{u}_d(s) \\ \tilde{i}_L(s) \end{bmatrix}$$

Though EKF is a very smart tool as a observer, there is a still delay in this dynamic, besides the sampling delay is also existed. In order to simplify the analysis, the EKF observer is equivalent to a time delay.

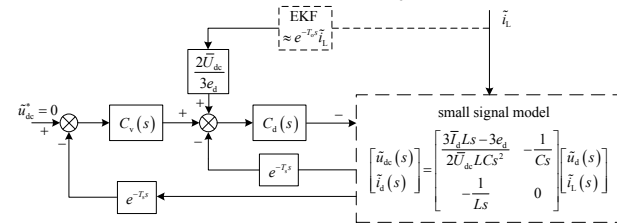


Fig. 4. the small-signal model with the feed-forward compensation

Fig.4 shows the small-signal model for the three-phase voltage-source PWM rectifier with the proposed control strategy. And the transfer function can be written as

$$(23) \quad \begin{bmatrix} \tilde{u}_{dc} \\ \tilde{i}_L \end{bmatrix} = \frac{2\bar{U}_d L s + \frac{2\bar{U}_d \bar{I}_d L s}{e_d} G_v(s) e^{-T_s} + 2\bar{U}_d G_v(s) e^{-T_s} - 2\bar{U}_d G_v(s) e^{-T_s}}{-\left(1 + \frac{1}{L s} e^{-T_s}\right) 2\bar{U}_d L C s^2 + 3(\bar{I}_d L s - e_d) e^{-T_s} G_d(s) G_v(s)}$$

It can be seen from Equation (23), the small dc-link voltage disturbance can be realized only if the recognition is fast enough. And when the observer time  $T_o$  is equal to the sample delay time  $T_s$ , the disturbance of the load current can almost be neglected.

### Simulation results

In order to verify the feasibility of the proposed control strategy, simulation studies were carried out under the conditions in Table 1.

Table 1. Parameters used in the three-phase voltage-source rectifier

Parameters	values
source voltage frequency/Hz	50
Source voltage line voltage (rms) /V	380
DC link voltage command/V	600
Inductance of reactor L/mH	3
Resistance of reactor R/ $\Omega$	0.15
DC link capacitor C/ $\mu$ F	1100
Switching frequency f/kHz	10
Load resistance $R_L$ / $\Omega$	66 $\rightarrow$ 37

The simulation model of the rectifier with the conventional controller shown in Fig.2 is made. The parameters of PI are selected with the voltage loop cut-off frequency as 200Hz, and the current loop cut-off frequency as 1000Hz.

The waveform of the dc voltage and the current of the A phase is shown in Fig. 5, when the load is changed from 66  $\Omega$  to 37  $\Omega$ .

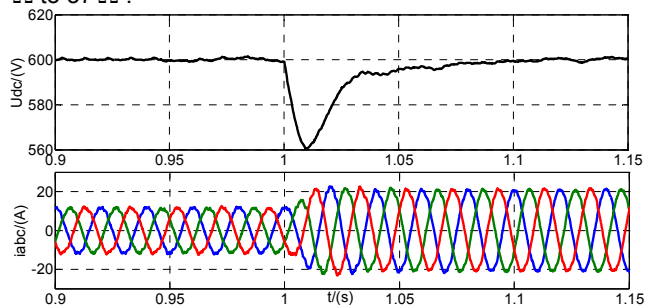


Fig.5.Simulation results with the conventional control strategy when the load resistant is changed from 66  $\Omega$  to 37  $\Omega$

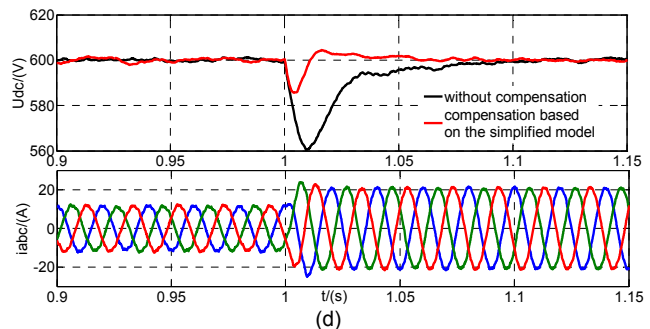
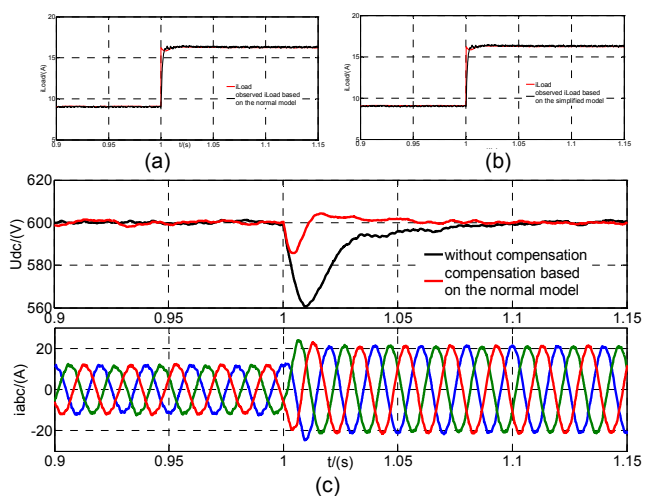


Fig.6.Simulation results the load resistant is changed from 66  $\Omega$  to 37  $\Omega$ . (a) The load current using EKF observer based on the normal model. (b) The load current using EKF observer based on the simplified model. (c) The dc-link voltage and ac current with/without EKF observer based on the normal model. (d) The dc-link voltage and ac current with/without EKF observer based on the simplified model

The real load current and the observed load current with EKF observers based on the normal rectifier model are shown in Fig. 6(a), without load current compensation. In Fig. 6(b), there are the real load current and the observed load current with EKF observers based on the simplified rectifier model. As can be seen, good static and dynamic performances of observers based on both the normal and simplified models can be gotten.

Fig. 6 (c) and (d) show the simulation results when the load resistant is changed from 66  $\Omega$  to 37  $\Omega$  (parallel connecting 66  $\Omega$  and 84  $\Omega$  resistant). As can be seen, the dc-link fluctuations with the compensations based on both the normal and simplified models are much smaller than that without compensation. The ac currents with the compensation based on the normal model are shown in Fig. 6 (c), and the ac currents with the compensation based on the simplified model are shown in Fig. 6 (d).

Both the dc-link voltage and ac current waves are almost the same, so the simplified mode can be instead of the normal model for EKF load current observing.

### Experimental system and results

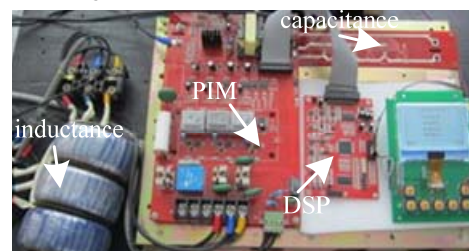


Fig.7.The three-phase voltage-source PWM rectifier controller

The experiment platform shown in Fig. 7 has also been set up, by taking the 32-bit TI TMS320F2808 DSP as central processing unit (CPU), Fuji seven unit PIM module 7MBR50SR120 as a power transmission unit, and a liquid crystal display (LCD) as a man-machine interface. The voltage is measured by the high-voltage probe connected the dc bus directly, and the ac current is measured by the current probe named Tektronix A622. The dead time of the system is set as 3  $\mu$ s, and the other main circuit parameters are the same with the simulation shown in Table. 1.

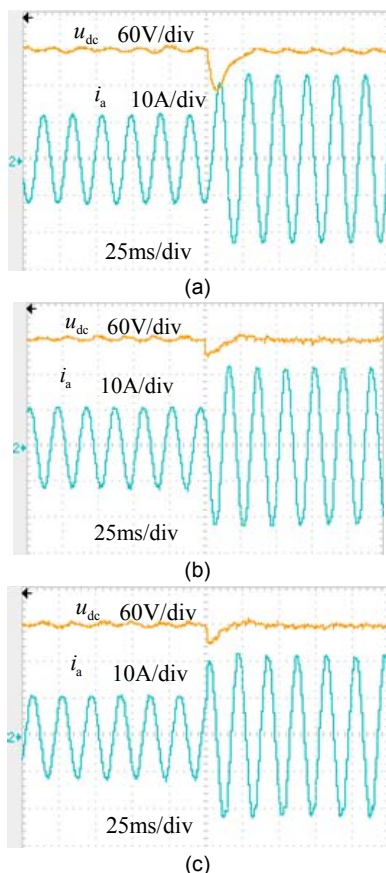


Fig.8. Experiment results when the load resistance changed from  $66\ \Omega$  to  $37\ \Omega$ . (a) Without compensation. (b) With compensation using EKF observer based on the normal model. (c) With compensation using EKF observer based on the simplified model

The experiment results with the direct current control strategy in d-q synchronous reference frame are shown in Fig. 8 (a). As can be seen, the dc-link voltage changed significantly when the load resistance jumped from  $66\ \Omega$  and then to  $37\ \Omega$ . Fig. 8 (b) shows the dc-link voltage and ac current using the feed-forward compensation strategy with EKF observer based on the normal model, and Fig. 8 (c) shows the dc-link voltage and ac current using the feed-forward compensation strategy with EKF observer based on the simplified model with the jumped load resistance. Fig. 8 (a), (b), and (c) show that, feed-forward compensation control strategy with both EKF observers based on the normal model and on the simplified one, can significantly reduce the voltage fluctuation to increase the anti-disturbance of the system. The compensation effect based on the simplified model can be nearly the same with the one based on the normal model.

## Conclusions

The feed-forward compensation control strategy using EKF observers based on both the normal and simplified models can be used to reduce the dc-link voltage fluctuation. And the compensation strategy based on the simplified model can realize nearly the same effect with the one based on the normal model. And the control strategy based on the simplified model may be more suitable for the industry application which always seeks low-cost.

The analysis method based on the small-signal model is also verified to be a useful method, which is suitable for other system's dynamic performance analysis. And other observer as long as the real-time requirement also can be used for the feed-forward compensation.

EKF observer used in this paper is very effective, which is also adapted to other dynamic demanding applications, such as the speed control system.

## REFERENCES

- [1] Bhim S., Brij N. S., Ambrish C., etc. A Review of Three-Phase Improved Power Quality AC-DC Converters. *IEEE Trans. Industrial Electronics*, 51(2004), No. 3, 641-660.
- [2] Akie U., Alok P., Tomonori G., etc. A Coordinated Control Method to Smooth Wind Power Fluctuation of a PMSG-Based WECS. *IEEE Trans. Energy Conversion*, 26(2011), No. 2, 550-558
- [3] ACS 600 Catalogue 2000 (EN 29.2.2000), ABB Automation Group Ltd., 2000.
- [4] Vector Control Simovet Masterdrives VC Catalog DA 65. 10 2003/2004, Siemens AG, Munich, Germany, 2000.
- [5] Mariusz M., Marek J., Marian P. K. Simple Direct Power Control of Three-Phase PWM Rectifier Using Space-Vector Modulation (DPC-SVM). *IEEE Trans. Industrial Electronics*, 51(2004), No. 2, 447-454
- [6] Jong-Woo C., Seung-Ki S.. Fast Current Controller in Three-Phase AC/DC Boost Converter Using d-q Axis Crosscoupling. *IEEE Trans. Power Electronics*, 13(1998), No. 1, 179-185
- [7] Namho H., Jinhwan J., Kwanghee N.. A Fast Dynamic DC-Link Power-Balancing Scheme for a PWM Converter-Inverter System. *IEEE Trans. Industrial Electronics*, 48(2001), No. 4, 794-803
- [8] Jinhwan J., Sunkyong L., Kwanghee N.. A Feedback Linearizing Control Scheme for a PWM Converter-Inverter Having a Very Small DC-Link Capacitor, *IEEE Trans. Industry Applications*, 35(1999), No. 5, 1124-1131
- [9] Bon-Gwan G., Kwanghee N.. A DC-Link Capacitor Minimization Method Through Direct Capacitor Current Control. *IEEE Trans. Industry Applications*, 42(2006), No. 2, 573-581
- [10] Luigi M., Leopoldo R., Paolo T., etc. AC/DC/AC PWM Converter with Reduced Energy Storage in the DC link. *IEEE Trans. Industry Applications*, 31(1995), No. 2, 287-292
- [11] Emanuele C., Alfio C., Angelo R., etc. A Robust Adaptive Controller for PM Motor Drives in Robotic Applications, *IEEE Trans. Power Electronics*, 10(1995), No. 1, 62-71
- [12] Ming-Fa T., Ying-Yu T.. A Transputer-Based Adaptive Speed Controller for AC Induction Motor Drives with Load Torque Estimation, *IEEE Trans. Industry Application*, 33(1997), No. 2, 558-566
- [13] Yongpeng Z., Cajetan M. A., Warsame H. A., etc. Load Disturbance Resistance Speed Controller Design for PMSM, *IEEE Trans. Industrial Electronics*, 53(2006), No. 4, 1198-1208
- [14] Sliverio B., Luca T., Mauro Z., Extended Kalman Filter Tuning in Sensorless PMSM Drives, *IEEE Trans. Industry Applications*, 39(2003), No. 6, 1741-1747
- [15] Yahia K., Zouzou S. E., Benchabane F., etc. Comparative study of an Adaptive Luenberger Observer and Extended Kalman filter for a Sensorless Direct Vector Control of Induction Motor, *Mediamira Science Publisher*, 50(2009), No. 2, 99-107
- [16] Peroutka Z., Smidl V., Vosmik D.. Challenges and limits of extended Kalman Filter based sensorless control of permanent magnet synchronous machine drives, in 13th European Conf. on Power Electronics and Applications (EPE'09), Barcelona, Spain, Sept.2009, pp: 1-11

**Authors:** Mr. Wang Ende, Room 6108, Electrical Machine Building, Institute of Electrical and Electronic Engineering, Huazhong University of Science and Technology, Wuhan City, Hubei Province, 430074, China, E-mail:wangende3321@163.com; prof. Huang Shenghua, Institute of Electrical and Electronic Engineering, Huazhong University of Science and Technology, Email: huangshh@163.com.